Articles

Penultimate Unit Effect in Ethene/Propene Copolymerization Promoted at High Temperature by Single Center Catalysts

Simona Losio,[†] Fabrizio Piemontesi,[‡] Fabrizio Forlini,[§] Maria Carmela Sacchi,[§] Incoronata Tritto,[§] Paola Stagnaro,[⊥] Gaetano Zecchi,[†] and Maurizio Galimberti*,[#]

Dipartimento di Scienze Chimiche e Ambientali, Università dell'Insubria, via Valleggio 11, 22100 Como, Italy; Basell Poliolefine Italia S.r.l., P.le Donegani 12, 44100 Ferrara, Italy; ISMAC-C.N.R., via E. Bassini 15, 20133 Milano, Italy; ISMAC-C.N.R. sez. Genova, via De Marini 6, 16149 Genova, Italy; and Pirelli Pneumatici, Viale Sarca 222, Milano 20162, Italy

Received June 8, 2006; Revised Manuscript Received September 20, 2006

ABSTRACT: This work reports on the microstructure of ethene/propene copolymers prepared in solution at high polymerization temperature with single center catalytic systems. Three different organometallic complexes were used as catalysts: a sterically hindered, highly regio- and stereo(iso)-specific metallocene, *rac*-[methylenebis-(3-*tert*-butyl-1-indenyl)]zirconium dichloride [*rac*-$H_2C-(3\text{-}^tBuInd)_2ZrCl_2$], the prototypical poorly isospecific hydrogenated metallocene without any substituent on the indenyl ligand, *rac*-ethylenebis(tetrahydroindenyl)-zirconium dichloride [*rac*-(EBTHI)$ZrCl_2$], and the so-called "constrained geometry" half-sandwich complex, {η^1:η^5-([*tert*-butylamido)dimethylsilyl](2,3,4,5-tetramethyl-1-cyclopentadienyl)}titanium dichloride [$Me_2Si(Me_4Cp)(N^tBu)TiCl_2$]. Copolymers microstructure was assessed through ^{13}C NMR analysis, and triad distribution data were elaborated through a statistical method that allows one to determine the reactivity ratios of the comonomers, r_1 and r_2. The product of reactivity ratios r_1r_2 of ethene/propene copolymers prepared with any of the catalysts increased to values higher than 1 when the copolymerization temperature was raised from 50 to 90 °C, thus indicating a *blocky* nature of the copolymers. Such an increase is due to different causes. The sterically hindered highly isospecific metallocene *rac*-$CH_2\text{-}(3\text{-}^tBu\text{-}Ind)_2ZrCl_2$, which at 50 °C already tends to produce blocky copolymers, increases its blockiness further on, mainly and surprisingly because of a remarkable r_2 increase. With [*rac*-(EBTHI)$ZrCl_2$], which at 50 °C tends to produce alternate copolymers, one observes a strong increase of r_1. With [$Me_2Si(Me_4Cp)(N^tBu)TiCl_2$] as well a remarkable increase of r_1 is obtained. Copolymerizations promoted by *rac*-$CH_2\text{-}(3\text{-}^tBu\text{-}Ind)_2ZrCl_2$ could be described by a second-order Markovian copolymerization model: the relative reactivity of ethene with respect to propene was found to decrease moving from EE to PE, to EP, and finally to PP as the last inserted monomeric units, and an inserted propene unit was thus found to bring about a higher propene reactivity also when it was in the penultimate position.

Introduction

Elastomers based on ethene and propene, the so-called polyolefin elastomers (POE), are an important presence in the field of synthetic rubbers.[1,2] In fact, they have an essentially saturated nature, with an ethene content from about 45% to about 70 mol % and only a minor amount of a diene, up to about 2−3 mol %, the double bond in the polymer being present not in the backbone chain but as a side group. This brings about an outstanding resistance of POE to aging and to atmospheric agents and is one of the main reasons for their relevant volume on the market: about 1 million tons at present, with a steadily increasing market share.

Elastomers based on ethene and propene were first prepared by Natta and his school, with the aim to reproduce the exceptional properties of natural rubber avoiding the problems brought about by double bonds.[3] A polymethylene chain was seen as the ideal one to have flexibility and the 1-olefin as the key to modulate crystallinity. In fact, in an ethene/propene elastomer, the way ethene and propene distribute themselves along the macromolecular chain and the nature of propene placement are the molecular features that control bulk properties and, in turn, the elastic behavior.[4]

Most of POE available on the commercial scale are produced with vanadium-based catalysts,[5,6] which prevent the formation of long ethene sequences and allow a remarkable degree of disorder in propene placement, thus giving rise to amorphous copolymers. Moreover, the single center nature of vanadium-based catalytic systems allows the preparation of homogeneous copolymer structures.[7]

A new generation of single center catalysts is nowadays employed on industrial scale for the preparation of ethene/propene elastomers, based either on metallocenes or on half-sandwich complexes, such as the so-called constrained geometry catalyst developed independently by Dow and Exxon.[8−23] Solution polymerizations are performed at very high tempera-

---

[†] Università dell'Insubria.
[‡] Basell Poliolefine Italia S.r.l..
[§] ISMAC-C.N.R.
[⊥] ISMAC-C.N.R. sez. Genova.
[#] Pirelli Pneumatici.
* To whom correspondence should be addressed: e-mail: maurizio.galimberti.ex@pirelli.com.

10.1021/ma0612780 CCC: $33.50

Table 1. E/P Copolymerization with Different Organometallic Complexes and MAO as the Catalytic System[a]

catalyst	run	f^b (mol/mol)	yield (g)	activity × 10^{-3} ($mg_{pol}/(mmol_{Mt}\ h)$)	$(E)_{copolym}{}^c$ (mol %)	monomer conversion (%)
rac-H_2C-(3-^{t}Bu-Ind)$_2ZrCl_2$	1	0.042	1.13	451.6	27.02	2.97
	2	0.078	0.55	281.4	42.81	1.17
	3	0.104	0.33	130.8	49.97	0.70
	4	0.176	2.00	802.8	73.79	2.43
rac-(EBTHI)$ZrCl_2$	5	0.042	1.27	507.2	44.47	2.61
	6	0.075	1.45	581.6	54.49	2.48
	7	0.099	0.77	310.0	66.45	1.00
[$Me_2Si(Me_4Cp)(N^tBu)TiCl_2$]	8	0.043	1.00	400.0	17.17	2.86
	9	0.078	0.97	387.6	22.54	2.72
	10	0.100	2.11	846.0	25.32	4.99
	11	0.152	1.51	603.2	33.82	3.36

[a] Polymerization conditions: toluene = 350 mL, Al/Mt = 1000 (mol/mol), T = 90 °C, [catalyst] = 10 μmol, and polymerization time = 15 min. [b] E/P feed ratio (mol/mol) in liquid phase. [c] From ^{13}C NMR analysis.

ture, thus exploiting all the typical advantages of this kind of technology.

However, studies on copolymers obtained at high temperature are rare in the literature, and thus this work was concentrated on crucial aspects of most recent developments of polyolefin elastomers, such as ethene/propene relative reactivity and distribution along the macromolecular chain and propene placement in copolymers prepared by single center catalysts at high polymerization temperature. Ethene/propene copolymerizations were performed at 90 °C, and comonomers relative reactivity and intramolecular distribution were expressed respectively by reactivity ratios r_1 and r_2 and by their product r_1r_2.

Single center catalysts representative of different values of reactivity ratio product (r_1r_2) for ethene/propene copolymerizations in a range of polymerization temperatures from 0 to 50 °C were selected: a sterically hindered, highly regio- and stereo-(iso)-specific metallocene, *rac*-[methylenebis(3-*tert*-butyl-1-indenyl)]zirconium dichloride [*rac*-H_2C-(3-^{t}BuInd)$_2ZrCl_2$],[24] discovered by L. Resconi for the synthesis of highly region and stereo(iso)-specific polypropene and able to promote E/P copolymerization at 50 °C with relatively high reactivity ratio product ($r_1r_2 = 1.8$),[25] the hydrogenated metallocene without any substituent on the indenyl ligand, *rac*-ethylenebis(tetrahydroindenyl)zirconium dichloride [*rac*-(EBTHI)$ZrCl_2$], which gives rise at 50 °C to relatively low reactivity ratio product ($r_1r_2 = 0.49$),[26a] and the so-called "constrained geometry " half-sandwich complex, {η^1:η^5-[(*tert*-butylamido)dimethylsilyl]-(2,3,4,5-tetramethyl-1-cyclopentadienyl)}titanium dichloride [$Me_2Si(Me_4Cp)(N^tBu)TiCl_2$],[27] with a reactivity ratio product very close to 1, which indicates a tendency of this catalyst to give a nearly random comonomer distribution. Copolymers were prepared in a wide range of chemical compositions and were carefully examined through ^{13}C NMR analysis; data on comonomer sequences, thus obtained, were elaborated through a statistical approach already successfully applied by some of the authors.[25−27]

Preliminary comments about the temperature effect on comonomer distribution are proposed, and thermal and crystallographic characterizations of ethene/propene copolymers prepared at 90 °C are given.

Results and Discussion

Synthesis and ^{13}C NMR Characterization. To investigate the effect of a high polymerization temperature on ethene/propene copolymer microstructure, copolymerizations were performed at 90 °C with single center catalysts representative of different values of reactivity ratio product (r_1r_2): [*rac*-H_2C-(3-^{t}BuInd)$_2ZrCl_2$] ($r_1r_2 = 1.8$),[25] [*rac*-(EBTHI)$ZrCl_2$] ($r_1r_2 = 0.49$),[26a] and $Me_2Si(Me_4Cp)(N^tBu)TiCl_2$ ($r_1r_2 = 1.1$).[27] In Table 1, data of E/P copolymerizations performed with the three catalysts and methylaluminoxane (MAO) as the cocatalyst are reported. Copolymerization conditions were optimized to obtain copolymer samples with homogeneous comonomer composition, suitable for microstructure investigation. In particular, to maintain nearly constant the comonomer concentration in solution throughout the whole course of the reaction, conversion of both comonomers was kept lower than 5%, following an experimental approach already reported by some of the authors.[25−27] A wide range of ethene/propene ratios in the polymerization bath was adopted and copolymers with an ethene content ranging from about 17 to about 73 mol % were prepared. Data arising from ^{13}C NMR analysis of the copolymers are collected in Table 2 for the two metallocene catalysts and in Table 3 for the constrained geometry catalyst.

Scheme 1

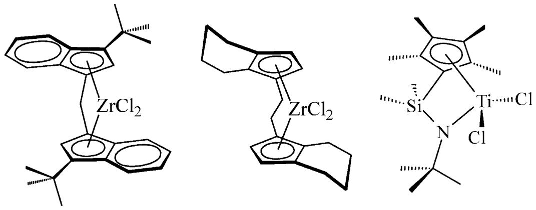

Ethene/propene copolymers prepared with the half-sandwich catalyst have a regioirregularity content ranging from 4.4 to 9.3 mol % for a molar ethene content of 33.8% and 17.2%, respectively. The presence of regioirregularities affects the determination of the triad distribution. However, their amount was considered low enough to regard as reliable the triad content shown in Table 3.

Determination of Reactivity Ratios of Comonomers. Triads of Tables 2 and 3 were elaborated with a method, already reported in a previous publication,[1a] that allows one to identify the statistical model suitable for describing the copolymerizations as well as for deriving the reactivity ratios between the comonomers. The reactivity ratios for ethene/propene copolymerizations were determined using a statistical approach based on Markovian copolymerization models. It is known that when the insertion of a comonomer is influenced by the last inserted unit (ultimate effect), a first-order Markovian statistical model is adopted to determine the reactivity ratios.[29] From the first Markovian model, r_1 (= k_{11}/k_{12}) and r_2 (= k_{22}/k_{21}) reactivity ratios are derived, where k_{ij} is the rate constant of the reaction for the addition of the monomer j to a growing chain bearing the comonomer i as the last inserted one. In particular, 1 and 2 indicate ethene and propene, respectively. In the literature, a first-order Markovian model has been used to describe E/P

Table 2. ^{13}C NMR Characterization of E/P Copolymers Prepared with Metallocenes and MAO as the Catalytic System

metallocene	sample no.[a]	f[b] (mol/mol)	$(E)_{copolym}$[c] (mol %)	PPP	PPE	EPE	PEP	PEE	EEE	regioirreg[d] (%)
rac-H_2C-(3-^{t}Bu-Ind)$_2$ZrCl$_2$	1	0.042	27.02	61.39	7.08	4.51	7.22	12.43	7.37	n.d.[e]
	2	0.078	42.81	34.42	15.60	7.16	6.36	18.12	18.33	n.d.[e]
	3	0.104	49.97	29.80	12.71	7.62	7.52	18.44	23.91	n.d.[e]
	4	0.176	73.79	9.51	8.52	8.19	3.10	21.13	49.55	n.d.[e]
rac-(EBTHI)ZrCl$_2$	5	0.042	44.47	22.46	20.25	12.83	14.98	21.40	8.09	n.d.[e]
	6	0.075	54.49	11.60	16.64	17.27	13.29	25.59	15.61	n.d.[e]
	7	0.099	66.45	7.68	9.62	16.26	8.38	27.68	30.39	n.d.[e]

[a] The numbers of the samples are those of the corresponding runs. [b] E/P feed ratio (mol/mol) in liquid phase. [c] From triad distribution as E = (PEP + EEP + EEE). [d] Calculated according to Randall[28] as $[100(^1/_2S\alpha\beta + {}^1/_2S\beta\gamma)/(S\alpha\alpha + {}^1/_2S\alpha\beta + S\beta\beta + {}^1/_2S\beta\gamma + S\gamma\gamma + {}^1/_2S\gamma\delta)$ from the ^{13}C NMR spectrum. [e] Not detectable.

Table 3. ^{13}C NMR Characterization of E/P Copolymers Prepared with "Constrained Geometry" Half-Sandwich Catalyst (III) and MAO as the Catalytic System[a]

sample no[b]	E (%)[c]	f[d] (mol/mol)	PPP	PPE	EPE	QEE	QEP	PEP	PEE	EEE	regioirreg[e] (%)
8	17.17	0.043	70.99	4.75	1.63	2.12	3.33	7.57	3.08	1.07	9.32
9	22.54	0.078	65.15	5.62	2.55	1.91	2.23	10.34	6.20	1.86	5.82
10	25.32	0.100	60.28	7.17	3.25	2.07	1.91	10.95	7.86	2.54	5.83
11	33.82	0.152	48.41	11.97	4.45	1.54	1.79	12.62	11.97	3.91	4.36

[a] Q = 2,1 propene inserted unit. [b] The numbers of the samples are those of the corresponding runs. [c] From triad distribution as E = (PEP + EEP + EEE). [d] E/P feed ratio (mol/mol) in liquid phase. [e] Calculated according to Randall[28] as $[100(^1/_2S\alpha\beta + {}^1/_2S\beta\gamma)/(S\alpha\alpha + {}^1/_2S\alpha\beta + S\beta\beta + {}^1/_2S\beta\gamma + S\gamma\gamma + {}^1/_2S\gamma\delta)$ from the ^{13}C NMR spectrum.

Table 4. Reactivity Ratios for E/P Copolymerizations with Different Organometallic Complexes and MAO as the Catalytic System

metallocene	T_{pol} (°C)	$r_1 \pm \delta r_1$	$r_2 \pm \delta r_2$	$r_1r_2 \pm \delta(r_1r_2)$[a]	ref
rac-H_2C-(3-^{t}Bu-Ind)$_2$ZrCl$_2$	50	17.4 ± 1.3	0.10 ± 0.02	1.8 ± 0.5	25
	90	29.0 ± 4.6	0.30 ± 0.05	8.8 ± 2.7	this work
rac-(EBTHI)ZrCl$_2$	50	10.4 ±0.7	0.05 ±0.01	0.5 ±0.1	26a
	90	18.5 ± 3.0	0.05 ± 0.01	1.0 ± 0.4	this work
[Me$_2$Si(Me$_4$Cp)(N^{t}Bu)TiCl$_2$]	50	1.3 ± 0.1	0.82 ± 0.05	1.1 ± 0.1	27
	90	3.8± 1.2	0.38 ± 0.04	1.4 ± 0.6	this work

[a] $\delta\ (r_1r_2) = r_1\delta r_2 + r_2\delta r_1$.

copolymerizations promoted by many different single center catalysts.[1] Nevertheless, it was reported by Fink,[30] by some of the authors,[1e,26a] and more recently by Busico[1k] and Kaminsky[1n,o] that metallocenes of the XInd$_2$MR$_2$ type (X = ethylene, Me$_2$Si, Me$_2$C) with either aromatic or hydrogenated C-6 ring fused on the Cp group promote E/P copolymerizations that can be better described by a second-order Markovian model; [*rac*-(EBTHI)ZrCl$_2$] is among these metallocenes. A second-order Markovian model describes a copolymerization when the insertion of a comonomer is influenced by the penultimate inserted unit (penultimate effect).[31] As a consequence of the adoption of the second-order Markovian model, the following reactivity ratios can be derived:

$$r_{11} = k_{111}/k_{112}$$

$$r_{21} = k_{211}/k_{212}$$

$$r_{22} = k_{222}/k_{221}$$

$$r_{12} = k_{122}/k_{121}$$

where k_{ijk} is the rate constant of the reaction for the addition of the monomer k to a growing chain bearing the comonomers i and j as the penultimate and the last (*ultimate*) inserted units, respectively. A better fitting of the experimental data with the second-order model has to be expected, as more reactivity ratios are employed. In the case of an evident better fitting, a "penultimate effect" can be claimed, as done by some of the authors for E/P copolymerizations with *rac*-(EBTHI)ZrCl$_2$-based catalyst at 50 °C.[1e,26a]

Both Markovian models were applied in the present work: as will be shown below, the interpretation of experimental data seems not to be affected by model selection. However, the second-order model allowed a better fitting and, in particular, a deeper insight into the mechanism of polymerizations promoted by *rac*-CH$_2$-(3-^{t}Bu-Ind)$_2$ZrCl$_2$.

In Table 4, r_1 and r_2 are collected together with the confidence intervals from the least squares at the minimum point and are compared with those reported in the literature for copolymerizations performed at 50 °C.[25−27] A general comparison among the reactivity ratios r_1 and r_2, at the two different polymerization temperatures, is also presented in the bar chart of Figure 1.

In general, $r_1 > r_2$, thus indicating that ethene insertion is preferred when either ethene or propene is the last inserted unit.

The stereorigid isospecific metallocene [*rac*-(EBTHI)ZrCl$_2$], which has no substituents on the indenyl ligands, promotes at 50 °C E/P copolymerizations characterized by r_1r_2 product lower than 1.[26a] The increase of copolymerization temperature causes a noticeable increase of r_1, whereas the r_2 value remains substantially unchanged. As a consequence, a higher value of r_1r_2 product is obtained; in fact, it moves from 0.5 ± 0.1 to 1.0 ± 0.4.

An r_1r_2 product higher than 1 (1.4) was also obtained with [Me$_2$Si(Me$_4$Cp)(N^{t}Bu)TiCl$_2$]. Analogously to what observed with [*rac*-(EBTHI)ZrCl$_2$], the increase of r_1r_2 product, as copolymerization temperature goes from 50 to 90 °C, is due to an increase of r_1. r_1r_2 products higher than 1 were also detected on commercial samples of POE prepared in solution at high polymerization temperature with a constrained geometry catalyst:[12−23] Table 5 shows r_1r_2 values for commercial grades Nordel IP 4770 and Nordel IP 3430.[32]

A different behavior by increasing polymerization temperature was observed with the stereorigid, sterically hindered, isospecific metallocene [*rac*-H$_2$C-(3-^{t}BuInd)$_2$ZrCl$_2$], which surprisingly

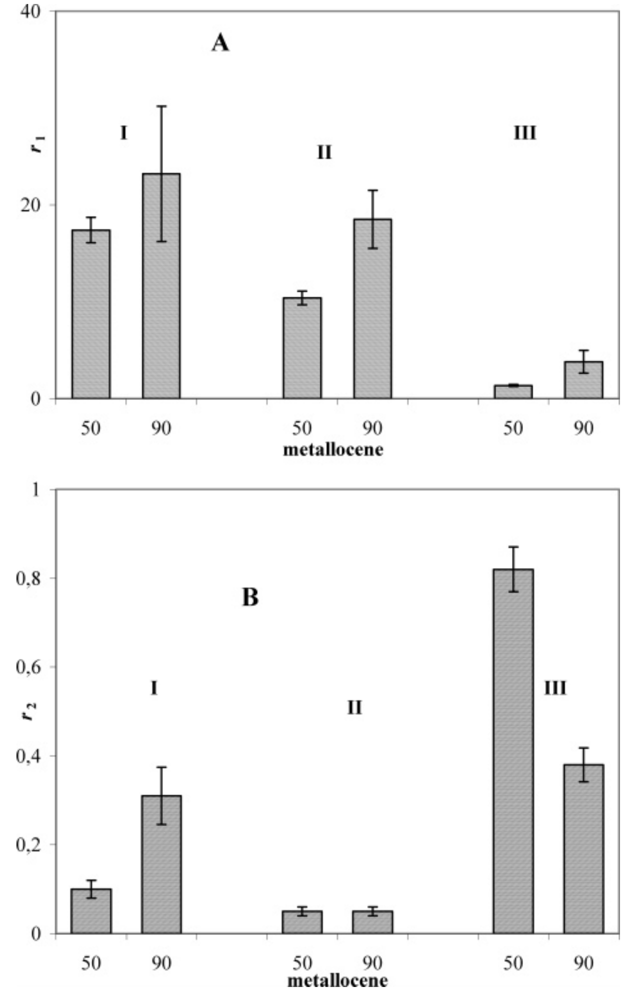

Figure 1. Reactivity ratios r_1 (A) and r_2 (B) of ethene/propene copolymerizations promoted by different organometallic complexes: [*rac*-H_2C-(3-^{t}BuInd)$_2$$ZrCl_2$] (**I**), [*rac*-(EBTHI)$ZrCl_2$] (**II**), and [Me_2Si-(Me_4Cp)(N^{t}Bu)$TiCl_2$], (**III**).

Table 5. Reactivity Ratios for Commercial Samples of POE Prepared in Solution at High Polymerization Temperature with "Constrained Geometry" Catalyst"[32]

	(P) (mol %)	propene sequences mm (mol %)	r_1r_2 [a]	regio-irregularities[b]
NORDEL IP 4770	18.8	20.1	1.84	3.3
NORDEL IP 3430	43.9	11.9	1.52	6.0

[a] From the ^{13}C NMR spectrum; see ref 33. [b] Calculated according to Randall[28] as $[100(^1/_2S\alpha\beta + ^1/_2S\beta\gamma)/(S\alpha\alpha + ^1/_2S\alpha\beta + S\beta\beta + ^1/_2S\beta\gamma + S\gamma\gamma + ^1/_2S\gamma\delta)$ from the ^{13}C NMR spectrum.

increases its tendency to promote sequences of both the comonomers; indeed, when the polymerization temperature changes from 50 to 90 °C, r_1 moves from 17.4 ± 1.3 to 29.0 ± 4.6, r_2 from 0.10 ± 0.02 to 0.30 ± 0.05 and r_1r_2 from 1.8 ± 0.5 to 8.8 ± 2.7. Thus, the higher value of r_1r_2 does not arise only from an increase of r_1 but also and interestingly from a noticeable increase of r_2 value. This means that, moving from ethene to propene as the last inserted unit, the increase of the polymerization temperature makes propene insertion less disfavored with respect to the ethene one.

To base these observations on parameters that could better fit the experimental data, triads of Table 2 were elaborated through a second-order Markovian model. In Table 6 are reported the values of the second-order Markovian reactivity ratios as well as the comonomer distribution index (CDI),[1e] i.e., an index based on second-order reactivity ratios and having the same meaning of the classical product of reactivity ratios r_1r_2 (e.g., CDI > 1 indicates a blocky copolymer), and it is useful to compare distributions generated from first- and second-order copolymerization statistics.

The CDI index obtained for *rac*-H_2C-(3-^{t}Bu-Ind)$_2$$ZrCl_2$ (CDI = 5.5 ± 1.8) is in line with the value of r_1r_2 = 8.8 ± 2.7 obtained from the first-order Markovian reactivity ratios and thus confirms the *blocky* nature of copolymers obtained with this metallocene. Analogously, the CDI value for copolymers from *rac*-(EBTHI)$ZrCl_2$ (CDI = 1.1 ± 0.2) indicates as well the increase of *blockiness*, already observed from r_1r_2 values, when 90 °C is the polymerization temperature. An evident improvement of data fitting was obtained not only, as expected, for copolymerizations promoted by *rac*-(EBTHI)$ZrCl_2$ but also, and interestingly, for copolymers from *rac*-H_2C-(3-^{t}BuInd)$_2$$ZrCl_2$, a metallocene that at 50 °C promotes E/P copolymerizations described by a first-order Markovian model. In both cases it is thus possible to hypothesize the occurring of a "penultimate" effect.

Moreover, it appears that with the sterically hindered stereorigid isospecific metallocene *rac*-H_2C-(3-^{t}BuInd)$_2$$ZrCl_2$, the high copolymerization temperature brings about a remarkable increase of reactivity ratios, such as r_2 and r_{22}, that indicate the formation of propene sequences. To investigate these noticeable findings, the ethene/propene relative reactivity was elaborated as a function of the two last inserted monomeric units.

Figure 2 shows the relative reactivity of ethene with respect to propene as a function of the chain end sequences, i.e., when the chain end sequences are EE, PE, EP, PP. It is evident that ethene relative reactivity decreases in the presence of last inserted sequences richer in propene, i.e., in the order EE-Zr, PE-Zr, EP-Zr, PP-Zr. As revealed by a comparison between corresponding runs (e.g., 1 and 5, 2 and 6, etc.) reported in Table 2, the ethene incorporation is lower for *rac*-H_2C-(3-^{t}BuInd)$_2$$ZrCl_2$ with respect to *rac*-(EBTHI)$ZrCl_2$, and the ethene reactivity for the former metallocene decreases as propene concentration in the feed increases.

In Figure 2, one can observe that the relative reactivity of ethene with respect to propene is higher when ethene is the last inserted monomeric unit, regardless of the penultimate inserted unit. This result clearly appears from the elaboration performed with both first- and second-order Markovian model. However, only the second-order Markovian model highlights the influence of the steric hindrance of the catalytic site. In fact, the relative reactivity of ethene with respect to propene decreases moving from EE to PE, to EP, and finally to PP as the last inserted monomeric units. It seems thus that a propene inserted unit has a relevant influence on the relative reactivity of the comonomers also when it is in the penultimate position, bringing about a higher propene reactivity.

So far, to our knowledge, only isospecific, sterically hindered metallocenes have been proven able to give rise to high r_1r_2 values in ethene/propene copolymerizations. In fact, a sterically hindered metallocene does not necessarily promote high values of r_1r_2 or r_2. As reported by some of the authors,[26b] *rac*-[ethylene-bis(4,7-dimethylindenyl)zirconium dichloride] [*rac*-(EBDMI)$ZrCl_2$] gives rise to r_1r_2 values higher than 1, whereas [*meso*-(EBDMI)$ZrCl_2$] gives rise to r_1r_2 values close to 0.2. The isospecificity of the catalyst is nevertheless not a sufficient condition to have copolymerization with a high product of reactivity ratios, as demonstrated also in this paper by the results obtained with [*rac*-(EBTHI)$ZrCl_2$]. Findings reported in the literature and in this paper could be tentatively interpreted by

Table 6. Reactivity Ratios Calculated Using a Second-Order Markovian Model for Ethene/Propene Copolymerizations with *rac*-H_2C-(3-^{t}Bu-Ind)$_2$ZrCl$_2$ (I) and *rac*-(EBTHI)ZrCl$_2$ (II)/Alumoxane as the Catalytic System[a]

metallocene	reactivity ratios[b]				CDI[c]
	r_{11}	r_{22}	r_{21}	r_{12}	
rac-H_2C-(3-^{t}Bu-Ind)$_2$ZrCl$_2$	25.8 ± 2.8	0.40 ± 0.05	19.4 ± 6.3	0.08 ± 0.02	5.5 ± 1.8
rac-(EBTHI)ZrCl$_2$	19.8 ± 1.7	0.09 ± 0.01	15.4 ± 1.8	0.03 ± 0.004	1.1 ± 0.2

[a] The experimental conditions are indicated in Table 1. [b] Calculated with the method described in ref 1a using a second-order Markovian model. [c] Comonomer distribution index calculated according to the formula CDI = $\sqrt{r_{11}{}^2 r_{22}{}^2 r_{12} r_{21}}$ (ref 1e).

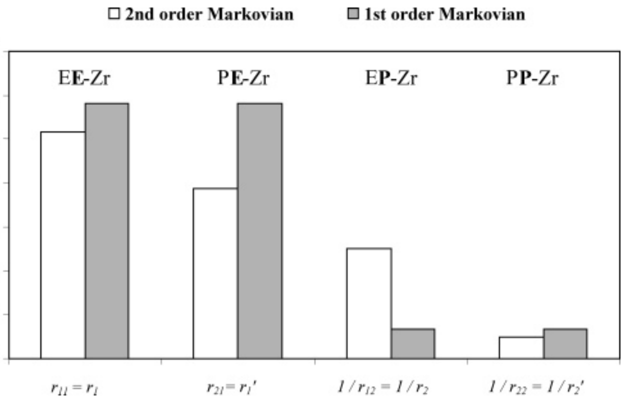

Figure 2. Comparison of ethene/propylene relative reactivity (r_1, r_1', $1/r_2$, and $1/r_2'$) obtained from first order ($r_1 = r_1'$ and $r_2 = r_2'$) and second order ($r_1 \neq r_1'$ and $r_2 \neq r_2'$) reactivity ratios for the copolymerizations promoted by [*rac*-H_2C-(3-^{t}BuInd)$_2$ZrCl$_2$]/MAO (**I**) (temperature of polymerization 90 °C).

the following considerations: (i) Only an isospecific metallocene can allow an easy propene propagation, to have the formation of propene sequences. (ii) The k_P for propene propagation of an isospecific site increases with the polymerization temperature and thus the r_{22} value increases. The increase of k_P with the polymerization temperature is higher than the increase of k_E, and thus the relative reactivity of propene increases as well. (iii) It is well-known that olefin insertion into a catalytic site is a result of the cooperation of the organometallic complex and of the growing chain. The role of inserted units in penultimate position is relevant indeed, as clearly indicated in the literature. For example, in 1-olefin hydrooligomerization reactions promoted by metallocene-based catalytic systems, enantiomeric excess for 1-olefin insertion remarkably increases from the first to the second addition of the monomer.[34,35] (iv) It seems that a metallocene, to be able to prepare ethene/propene copolymers with a high product of reactivity ratios, should be endowed with a high isospecificity, to a level that is not clear at the moment. Lack of isoselectivity in propene placement, to a minor extent as in the case of *rac*-(EBTHI)ZrCl$_2$ or to a large extent as in the case of [Me$_2$Si(Me$_4$Cp)(N^{t}Bu)TiCl$_2$], seems thus to be responsible for the different values of reactivity ratios.

Thermal Characterization of Copolymers from *rac*-H_2C-(3-^{t}BuInd)$_2$ZrCl$_2$. In an ethene/propene copolymer with a high product of reactivity ratios prepared with an isospecific catalyst long sequences of both comonomers are able to crystallize.[36] The thermal behavior of copolymers from the highly isospecific metallocene *rac*-H_2C-(3-^{t}BuInd)$_2$ZrCl$_2$, which present long sequences of both comonomers, was investigated. Melting enthalpies of samples 1−4, having widely different compositions (27−74 mol % of ethene), are reported in Table 7.

Table 7. Thermal Characterization of E/P Copolymers with *rac*-H_2C-(3-^{t}Bu-Ind)$_2$ZrCl$_2$/MAO (I) as the Catalytic System[a]

run	(E)$_{copolym}$[b] (mol %)	T_c[c] (°C)	T_g[d] (°C)	T_m[d] (°C)	ΔH_m[d] (J/g)
1	27.02	72.2	−43.9	107.8	18.65
2	42.81	70.2	−49.2	107.1	7.33
3	49.97		−32.7		
4	73.79	47.6	−45.2	63.5	41.6

[a] The experimental conditions are indicated in Table 1. [b] From triad distribution as E = (PEP + EEP + EEE). [c] Determined on controlled cooling. [d] Determined on second heating.

Sample 4 shows a higher enthalpy of fusion (41.6 J/g) as a consequence of the presence of crystalline ethene sequences, as confirmed by WAXD analysis. Sample 3 with an ethene content of 49.97% can be considered as truly amorphous. In fact, its DSC heating curve does not present any endothermic peak but only a well-defined glass transition located at −32.7 °C. Both samples 1 and 2 show melting peaks at about 107 °C with related enthalpy which decreases at increasing ethene content in the copolymers (14.65 and 7.33 J/g, respectively). X-ray diffractograms of samples 1 and 2 show the typical reflections of the α modification of isotactic polypropene, although the peaks at higher 2θ° values are not well-defined. Thus, we can conclude that in copolymers with a high product of reactivity ratios and isotactic propene sequences, as those prepared with *rac*-H_2C-(3-^{t}BuInd)$_2$ZrCl$_2$, crystallinity due to both comonomers can be detected in a wide range of chemical compositions.

Experimental Section

General Remarks. Manipulations of air- and/or moisture-sensitive materials were carried out under an inert atmosphere using a dual vacuum/nitrogen line and standard Schlenk techniques or in a drybox under a nitrogen atmosphere (<10 ppm oxygen, <20 ppm water). Toluene was dried by distillation from sodium under a nitrogen atmosphere. Methylaluminoxane (MAO) (Witco, 10 wt % solution in toluene) was used after drying in a vacuum to remove the solvent and unreacted trimethylaluminum (TMA) and was stored under nitrogen. Nitrogen and propene were purified by passage through columns of BASF RS-11 (Fluka) and Linde 4 Å molecular sieves.

Determination of the Concentration of the Polymerization Solutions. The vapor−liquid equilibrium for E/P toluene mixture was calculated from the Redlich−Kwong−Soave equations.[37] This set of thermodynamic equations was selected among those available in Aspen Plus (commercialized by Aspen Technology Inc. Release 9) on the basis of a comparison with the experimental results. The concentrations of the comonomers were hence calculated.

Ethene/Propene Polymerizations. In a typical polymerization reaction, a 1 L Büchi autoclave equipped with a mechanical stirrer was charged under nitrogen with a solution of 7.5 mmol of dry methylaluminoxane (MAO) in 330 mL of anhydrous toluene, and then 30 g of propene was added. A 25 mL injector was charged with 10 mL of a solution of 10 μmol of catalyst and 2.5 mmol of MAO in toluene (total MAO/Mt ratio = 1000). After thermal equilibration of the reactor system at 90 °C, ethene was continuously added until saturation. When the equilibrium pressure (0.8, 1.5, and 2 atm of overpressure) was reached, the injector with the metallocene solution was pressurized with nitrogen, and the solution was injected into the reactor. The solution was stirred for 15 min. The reaction was terminated by addition of a small amount of ethanol, and the polymer was precipitated upon pouring the whole reaction mixture into ethanol (800 mL), to which concentrated hydrochloric acid (5 mL) had been added. The polymer was collected by filtration and dried under vacuum at 70 °C.

Nuclear Magnetic Resonance (NMR). ^{13}C NMR spectra of the polymers were recorded in $C_2D_2Cl_4$ at 103 °C on a Bruker AM-400 spectrometer operating at 100.58 MHz (internal chemical shift reference: 1% hexamethyldisiloxane). Conditions: 10 mm probe; 90° pulse angle; 64K data points; acquisition time 5.56 s; relaxation delay 20 s; 3K−4K transients. Proton broad-band decoupling was achieved with a 1D sequence using bi_waltz16_32 power-gated decoupling.

Thermal Analysis. Differential scanning calorimetry (DSC) scans were carried out on a Mettler DSC 821^e instrument under a nitrogen atmosphere. Typically, ca. 5 mg of polymer was heated to 180 °C and held at this temperature for 3 min to cancel previous thermal history. The specimens were then cooled under controlled conditions (20 °C/min) up to −100 °C to reveal the crystallization behavior. Subsequently, a second heating run, up to 180 °C with a scan rate of 20 °C/min, was imposed to determine the melting transition and the enthalpy of fusion.

X-ray Analysis. The wide-angle X-ray diffraction (WAXD) data were obtained at 20 °C using a Siemens D-500 diffractometer equipped with a Siemens FK 60-10 2000 W tube (Cu Kα radiation, $\lambda = 0.154$ nm); operating voltage = 40 kV; current = 40 mA. The data were collected from 5 to 30 $2\theta°$ at 0.02 $2\theta°$ intervals.

Acknowledgment. The authors are deeply grateful to Dr. L. Resconi for generous donation of *rac*-H_2C-(3-^{t}BuInd)$_2ZrCl_2$ catalyst. They warmly thank Mr. G. Zannoni, who has carefully and expertly performed all the NMR spectra, and Mr. M. Canetti for his helpful contribution to X-ray analyses. Dr. P. Locatelli's intellectual and experimental contributions are also gratefully acknowledged.

References and Notes

(1) (a) Galimberti, M.; Piemontesi, F.; Fusco, O.; Camurati, I.; Destro, M. *Macromolecules* **1998**, *31*, 3409−3416. (b) Kravchenko, R.; Waymouth, R. M. *Macromolecules* **1998**, *31*, 1−6. (c) Polo, E.; Galimberti, M.; Mascellani, N.; Fusco, O.; Mueller, G.; Sostero, S. *J. Mol. Catal. A: Chem.* **2000**, *160*, 229−236. (d) Kim, L. D. *J. Polym. Sci., Part A: Polym. Chem.* **2000**, *38*, 1427−1432. (e) Galimberti, M.; Piemontesi, F.; Baruzzi, G.; Mascellani, N.; Camurati, I.; Fusco, O. *Macromol. Chem. Phys.* **2001**, *202*, 2029−2037. (f) Kaminsky, W. *Macromol. Symp.* **2001**, *174*, 269−276. (g) Fan W.; Leclerc, M. K.; Waymouth, R. M. *J. Am. Chem. Soc.* **2001**, *123*, 9555−9563. (h) Fan, W.; Waymouth, R. M. *Macromolecules* **2001**, *34*, 8619−8625. (i) Longo, P.; Siani, E.; Pragliola, S.; Monaco, G. *J. Polym. Sci., Part A: Polym. Chem.* **2002**, *40*, 3249−3255. (j) Reybuck, S. E.; Meyer, A.; Waymouth, R. M. *Macromolecules* **2002**, *35*, 637−643. (k) Busico, V.; Cipullo, R.; Segre, A. L. *Macromol. Chem. Phys.* **2002**, *203*, 1403−1412. (l) Hung, J.; Cole, A. P.; Waymouth, R. M. *Macromolecules* **2003**, *36*, 2454−2463. (m) Reybuck, S. E.; Waymouth, R. M. *Macromolecules* **2004**, *37*, 2342−2347. (n) Karssenberg, F. G.; Piel, C.; Hopf, A.; Mathot, V. B. F.; Kaminsky, W. *J. Polym. Sci., Part B: Polym. Phys.* **2005**, *44*, 747−755. (o) Karssenberg, F. G.; Wang, B.; Friederichs, N.; Mathot, V. B. F. *Macromol. Chem. Phys.* **2005**, *206*, 1675−1683. (p) Piel, C.; Karssenberg, F. G.; Kaminsky, W.; Mathot, V. B. F. *Macromolecules* **2005**, *38*, 6789−6795. (q) Tynys, A.; Saarinen, T.; Hakala, K.; Helaja, T.; Vanne, T.; Lehmus, P.; Loefgren, B. *Macromol. Chem. Phys.* **2005**, *206*, 1043−1056. (r) Heuer, B, Kaminsky, W. *Macromolecules* **2005**, *38*, 3054−3059. (s) Baughman, T. W.; Sworen, J. C.; Wagener, K. B. *Macromolecules* **2006**, *39*, 5028−5036.

(2) Older papers on ethene/propene copolymerization promoted by metallocene catalysts are collected in ref 5 of ref 1a.

(3) Natta, G.; Mazzanti, G.; Valvassori, A.; Sartori, G.; Morero, D. *Chim. Ind. (Milan)* **1960**, *42*, 125−132.

(4) Guerra, G.; Galimberti, M.; Piemontesi, F.; Ruiz de Ballesteros, O. *J. Am. Chem. Soc.* **2002**, *124*, 1566−1567.

(5) Natta, G.; Pasquon, I.; Zambelli, A. *J. Am. Chem. Soc.* **1962**, *84*, 1488−1490.

(6) (a) Zambelli, A.; Locatelli, P.; Bajo, G.; Bovey, F. A. *Macromolecules* **1975**, *8*, 687−689. (b) Zambelli, A.; Sessa, I.; Grisi, F.; Fusco, R.; Accommazzi, P. *Macromol. Chem., Rapid Commun.* **2001**, *22*, 297−310.

(7) (a) Zucchini, U.; Dall'Occo, T.; Resconi, L. *Indian J. Technol.* **1993**, *31*, 247−262 and references therein. (b) Galimberti, M.; Martini, E.; Piemontesi, F.; Sartori, F.; Resconi, L.; Albizzati, E. *Macromol. Symp.* **1995**, *89*, 259−275.

(8) McKnight, A.; Waymouth, R. M. *Chem. Rev* **1998**, *98*, 2587−2598 and references therein.

(9) Okuda, J. *Chem. Ber.* **1990**, *123*, 1649−1651.

(10) (a) Canich, J. A. M. (Exxon). U.S. Patent 5,026,798, 1991. (b) Canich, J. A. M.; Licciardi, G. F. (Exxon). U.S. Patent 5,057,475, 1991. (c) Canich, J. A. M. (Exxon). Eur. Pat. Appl. 0420 436 A1, 1991. (d) Stevens, J. C.; Timmers, F. J.; Wilson, D. R.; Schmidt, G. F.; Nickias, P. N.; Rosen, R. K.; Knight, G. W.; Lai, S.-y. (Dow). Eur. Pat. Appl. 0 416 815 A2, 1991. (e) Stevens, J. C.; Neithamer, D. R. (Dow). Eur. Pat. Appl. 0 418 044 A2, 1991.

(11) (a) Knight, G. W.; Maugans, R. A.; Knickerbocker, E. N. PCT Int. Appl. WO 94-25647, 1994. (b) McKay, K. W.; Banchard, R. R.; Feig, E. R.; Kummer, K. G. PCT Int. Appl. WO. 94-06856, 1994.

(12) Pannell, R. B.; Canich, J. A. M.; Hlatky, G. G. (Exxon). PCT Int. Appl. WO 94/00500, 1994.

(13) Canich, J. A. M. (Exxon). U.S. Patent 5,096,867, 1992.

(14) Brant, P.; Canich, J. A. M. (Exxon). PCT Int. Appl. WO 93/12151, 1993.

(15) Brant, P.; Canich, J. A. M.; Merrill, N. A. (Exxon). PCT Int. Appl. WO 93/21242, 1993.

(16) Brant, P.; Canich, J. A. M.; Dias, A. J.; Bamberger, R. L.; Licciardi, G. F.; Henrichs, P. M. (Exxon). PCT Int. Appl. 94/07930, 1994.

(17) Canich, J. A. M. (Exxon). PCT Int. Appl. WO 96/00244, 1996.

(18) LaPointe, R. E.; Rosen, R. K.; Nickias, P. N. (Dow). Eur. Pat. Appl. 0 495 375 A2, 1992.

(19) LaPointe, R. E.; Stevens, J. C.; Nickias, P. N.; McAdon, M. H. (Dow). Eur. Pat. Appl. 0 520 732 A1, 1992.

(20) Lai, S. Y.; Wilson, J. R.; Knight, G. W.; Stevens, J. C. (Dow). PCT Int. Appl. WO 93/08221, 1993.

(21) Rosen, R. K.; Nickias, P. N.; Devore, D. D.; Stevens, J. C.; Timmers, F. J. (Dow). U. S. Patent 5,374,696, 1994.

(22) Devore, D. D.; Crawford, L. H.; Stevens, J. C.; Timmers, F. J.; Mussell, R. D.; Wilson, D. R.; Rosen, R. K. (Dow). PCT Int. Appl. WO 95/00526, 1995.

(23) Nickias, P. N.; McAdon, M. H.; Patton, J. T. (Dow). PCT Int. Appl. WO 97/15583, 1997.

(24) Resconi, L.; Balboni, D.; Baruzzi, G.; Fiori, C.; Guidotti, S. *Organometallics* **2000**, *19*, 420−429.

(25) Locatelli, P.; Losio, S.; Forlini, F.; Sacchi, M. C.; Tritto, I.; Galimberti, M.; Piemontesi, F. Communication at "European Polymer Conference on Stereospecific Polymerization and Stereoregular Polymers"-EUPOC 2003, Milano, Italy, 8−12 June, 2003.

(26) (a) Galimberti, M.; Destro, M.; Fusco, O.; Piemontesi, F.; Camurati, I. *Macromolecules* **1999**, *32*, 258−263. (b) Galimberti, M.; Piemontesi, F.; Mascellani, N.; Camurati, I.; Fusco, O.; Destro, M. *Macromolecules* **1999**, *32*, 7968−7976.

(27) Galimberti, M.; Mascellani, N.; Piemontesi, F.; Camurati, I. *Macromol. Rapid Commun.* **1999**, *20*, 214−218.

(28) Randall, J. C. *Macromolecules* **1978**, *33*, 11−13.

(29) Odian, G. *Principles of Polymerization*, 3rd ed.; Wiley & Sons: New York, 1991; pp 455−458.

(30) Herfert, N.; Montag, P.; Fink, G. *Makromol. Chem.* **1993**, *194*, 3167−3182.

(31) Odian, G. *Principles of Polymerization*, 3rd ed.; Wiley & Sons: New York, 1991; pp 503−505.

(32) (a) Nordel IP 4770 and Nordel IP 3430 are trademarks of The Dow Chemical Company (Dow) or an affiliated company of Dow. (b) Galimberti, M. EP(D)M Elastomers presented at Elastomers 2001, First EPF School, XXIII M. Farina-AIM School, Gargnano (BS) (I), June 4−8, 2001; unpublished results.

(33) Carman, C. J.; Wilkes, C. E. *Rubber Chem. Technol.* **1971**, *44*, 781−804.

(34) Pino, P.; Galimberti, M.; Prada, P.; Consiglio, G. *Makromol. Chem.* **1990**, *191*, 1677−1688.

(35) Zambelli, A.; Sacchi, M. C.; Locatelli, P.; Zannoni, G. *Macromolecules* **1982**, *15*, 211−212.

(36) See for instance ref 4 and references therein.

(37) (a) Soave, G. *Chem. Eng. Sci.* **1972**, *27*, 1197−1203. (b) Peneloux, A.; Rauzy, E.; Freze, R. *Fluid Phase Equilib.* **1982**, *8*, 7−23. (c) Schwartzentruber, J.; Renon, H. *Ind. Eng. Chem. Res.* **1989**, *28*, 1049−1055.

MA0612780